Developmental Cell
Article

Dynamin Participates in the Maintenance of Anterior Polarity in the *Caenorhabditis elegans* Embryo

Yuji Nakayama,[1,3,4] Jessica M. Shivas,[1,3] Daniel S. Poole,[1] Jayne M. Squirrell,[2] Jennifer M. Kulkoski,[1] Justin B. Schleede,[1] and Ahna R. Skop[1,*]
[1]Department of Genetics
[2]Laboratory for Optical and Computational Instrumentation
University of Wisconsin-Madison, Madison, WI 53706, USA
[3]These authors contributed equally to this work
[4]Present address: Department of Molecular Cell Biology, Graduate School of Pharmaceutical Sciences, Chiba University, Chiba 260-8675, Japan
*Correspondence: skop@wisc.edu
DOI 10.1016/j.devcel.2009.04.009

SUMMARY

Cell polarity is crucial for the generation of cell diversity. Recent evidence suggests that the actin cytoskeleton plays a key role in establishment of embryonic polarity, yet the mechanisms that maintain polarity cues in particular membrane domains during development remain unclear. Dynamin, a large GTPase, functions in both endocytosis and actin dynamics. Here, the *Caenorhabditis elegans* dynamin ortholog, DYN-1, maintains anterior polarity cues. DYN-1-GFP foci are enriched in the anterior cortex in a manner dependent on the anterior polarity proteins, PAR-6 and PKC-3. Membrane internalization and actin comet formation are enriched in the anterior, and are dependent on DYN-1. PAR-6-labeled puncta are also internalized from cortical accumulations of DYN-1-GFP. Our results demonstrate a mechanism for the spatial and temporal regulation of endocytosis in the anterior of the embryo, contributing to the precise localization and maintenance of polarity factors within a dynamic plasma membrane.

INTRODUCTION

Cell polarity is crucial for generating diversity throughout development. In the *Caenorhabditis elegans* embryo, polarity is determined by opposing PAR protein complexes that create distinct anterior and posterior domains (Cuenca et al., 2003; Goldstein and Macara, 2007). The PAR-6/PAR-3/PKC-3 complex localizes to the anterior cortex. PAR-2, on the other hand, localizes to the posterior cortex by an exclusion mechanism mediated by PAR-3 and CDC-42 (Boyd et al., 1996). Ultimately, the generation of cellular asymmetry along the anterior-posterior axis leads to proper spindle alignment and segregation of cytoplasmic determinants into newly formed daughter cells (Cheeks et al., 2004; Munro, 2006; Severson and Bowerman, 2003).

In the *C. elegans* one-celled embryo, there are two distinct phases of polarity: establishment and maintenance. These phases are regulated by the small GTPases, RHO-1 and CDC-42, respectively (Aceto et al., 2006; Cowan and Hyman, 2007; Goldstein and Macara, 2007; Motegi and Sugimoto, 2006). Acto-myosin contractility, which is regulated by RHO-1 and generates the cortical flow, is responsible for the establishment of polarity (Motegi and Sugimoto, 2006; Munro et al., 2004; Schonegg and Hyman, 2006). In contrast, mechanisms to maintain the established asymmetry remain unclear. Accumulating evidence and mathematical models suggest that polarized protein distributions require a balance of diffusion, membrane transport, and endocytosis (Altschuler et al., 1999; Andrews and Ahringer, 2007; Emery and Knoblich, 2006; Harris and Tepass, 2008; Marco et al., 2007; Vanzo et al., 2007). Additionally, anterior polarity factors, such as PAR-6 and CDC-42, can specifically regulate endocytic machinery in *C. elegans* coelomocytes (Balklava et al., 2007). Current models propose that PAR proteins could regulate membrane recycling to generate or possibly maintain a plasma membrane domain and boundary in the one-celled embryo (Wissler and Labouesse, 2007); however, the links between polarity maintenance and endocytosis in the *C. elegans* one-celled embryo have not been identified.

Dynamins are large GTPases involved in a variety of cellular processes, including clathrin-mediated endocytosis, membrane remodeling, actin recruitment, and actin-based vesicle motility (Hinshaw, 2000; Orth and McNiven, 2003; Schafer, 2004). Several dynamin homologs and isoforms play roles in generating cellular asymmetry or interacting with factors responsible for doing so. In *Drosophila*, the loss of dynamin (Shibire) perturbs Wingless distribution in the endoderm (Bejsovec and Wieschaus, 1995) and Decapentaplegic (Dpp) signal transduction within the wing disc epithelium (Entchev et al., 2000). Recently, the dynamin-associated protein, Dap160/intersectin, has been identified as a binding partner of aPKC, functioning in the regulation of cell polarity of *Drosophila* neuroblasts (Chabu and Doe, 2008). Dynamin, Cdc42, and Arp2/3-dependent endocytic mechanisms were found to be crucial in the maintenance of junctional stability in epithelial cells (Georgiou et al., 2008; Leibfried et al., 2008). In mammals, two dynamin isoforms appear to have specific roles in targeting vesicles to either the apical or the basolateral surface in Madine-Darby canine kidney cells (Altschuler et al., 1998). Clathrin is required for proper targeting of basolateral proteins

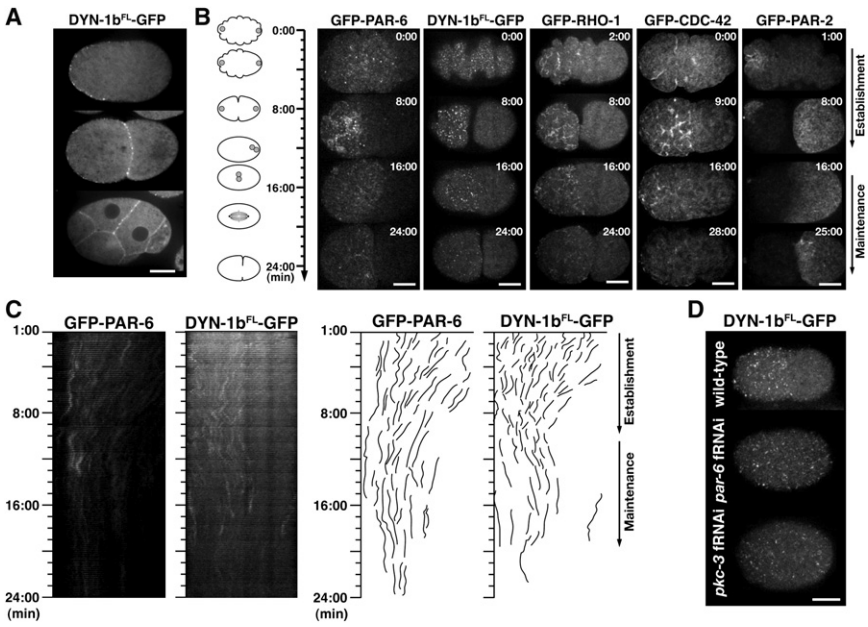

Figure 1. Dynamin Localizes to the Anterior Cortex of the One-Celled Embryo in a PAR-6-Dependent Manner

(A) DYN-1b^{FL}-GFP localizes to anterior cortex, cortex of AB cell, and newly formed membrane.

(B) (Left) Schematic representations of cell cycle progression. (Right) Cortical images of GFP-PAR-6, DYN-1b^{FL}-GFP, GFP-RHO-1, GFP-CDC-42, and GFP-PAR-2. Times (min) are with respect to the onset of cortical flow.

(C) (Left) Kymographs of GFP-PAR-6 or DYN-1b^{FL}-GFP-expressing embryos (see Experimental Procedures). (Right) The isointensity lines in kymograph were traced manually.

(D) Cortical images of DYN-1b^{FL}-GFP are shown in WT and *par-6*- or *pkc-3*-fRNAi-treated embryos. Anterior is to the left. Scale bars, 10 μm.

in epithelial cells (Deborde et al., 2008). While dynamin has been implicated in numerous events involving regulation of polarity, little is known about the role(s) of dynamin during embryonic development.

In this study, we have uncovered mechanisms required to maintain anterior polarity factors in the plasma membrane in developing *C. elegans* embryos. We show that dynamin is critical for the maintenance of anterior cell polarity in the *C. elegans* embryo by regulating endocytic events.

RESULTS

DYN-1 Is Required for Anterior Spindle Pole Movements

In wild-type (WT) embryos, the spindle poles move asymmetrically toward the posterior (Albertson, 1984). We discovered a subtle but consistent aberrant anterior spindle displacement in *dyn-1* feeding RNAi-treated embryos (fRNAi) (see Figure S1 available online) similar to those observed in the embryos depleted for the polarity-regulating proteins, PAR-3, PAR-2, RHO-1, or CDC-42 (Grill et al., 2001; Motegi and Sugimoto, 2006). This result indicates a disruption of polarity in the *dyn-1* fRNAi-treated embryos. Since DYN-1 depletion by fRNAi leads to sterility and embryonic lethality (Thompson et al., 2002), the polarity defects that we observed were due to partially depleting DYN-1 protein (see Experimental Procedures and Figure S2). Under these conditions, we still observed sterility and embryonic lethality (74% fewer embryos were produced and the lethality within the produced embryos was 13%). Due to the partial nature of the DYN-1 depletion, all of the phenotypes observed should be considered hypomorphs.

DYN-1 Foci Localize to the Anterior Cortex of the Embryo

We observed an enrichment of endogenous DYN-1 at the anterior cortex of one-celled embryos (Figure S3), in addition to the cleavage furrow and midbody accumulation reported previously (Thompson et al., 2002). To determine the dynamics of DYN-1 during anterior-posterior axis formation, transgenic strains expressing GFP-fused full-length DYN-1 isoform b (DYN-1b^{FL}-GFP, also referred to as DYN-1-GFP) were generated. The mid-focal plane images showed that DYN-1b^{FL}-GFP localized to the anterior cortex and newly formed furrow membrane (Figure 1A), as observed for the endogenous DYN-1. To analyze the dynamics at the cortex, time-lapse recordings were taken from the onset of cortical flow (Figures 1B and 1C, 0:00 min) to cleavage furrow formation (around 24:00 min). Differences in cortical and cytoplasmic flows during the first cell cycle have been previously characterized (Cuenca et al., 2003; Hird and White, 1993; Munro et al., 2004) and serve as markers for the distinct phases of polarity (Cuenca et al., 2003; Motegi and Sugimoto, 2006; Velarde et al., 2007). The time-lapse images of DYN-1-GFP-expressing embryos were then compared with that of embryos expressing GFP-fusion proteins of known polarity factors. GFP-PAR-6 spans the entire cortex at the onset of the cortical flow (Figure 1B, 0:00 min), then moves anteriorly along with the cortical flow, segregating to the anterior half prior to pseudocleavage (Figures 1B and 1C, 8:00 min, polarity establishment phase), as described previously (Cuenca et al., 2003; Munro et al., 2004). PAR-2 was observed at low levels at the cortex just before polarization (Figure 1B, 1:00 min), and accumulated at the posterior end of the embryo after spreading to occupy around one-half of the entire embryo (Figure 1B, 8:00 min) (Cuenca et al., 2003). After the establishment phase (~8:00 min), the polarized localization of both PAR-6 and PAR-2 was maintained throughout pronuclear meeting, centration, and rotation. Two small GTPases, RHO-1 and CDC-42, tagged with GFP, were enriched to the anterior cortex (Figure 1B), as described previously (Motegi and Sugimoto, 2006). We found that DYN-1b^{FL}-GFP was distributed throughout the entire cortex as small punctate foci prior to polarity establishment (Figure 1B, 0:00 min), moving anteriorly during cortical flows (Figures 1B and 1C). By pseudocleavage, DYN-1b^{FL}-GFP foci were confined to the anterior half (Figures 1B and 1C, 8:00 min). This anterior localization was maintained throughout mitosis, similar to the localization of GFP-PAR-6.

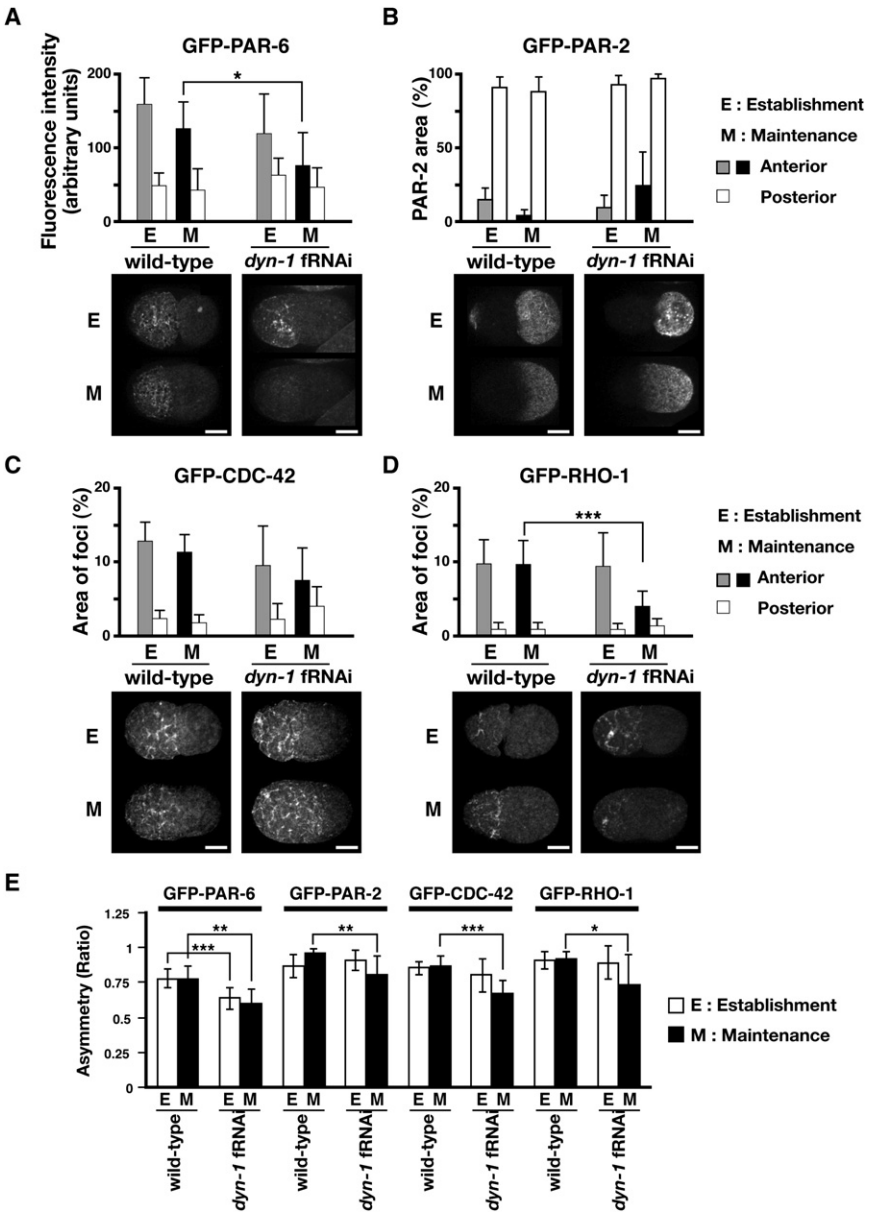

Figure 2. Depletion of DYN-1 Affects Polarity Maintenance

(A) GFP-PAR-6-, (B) GFP-PAR-2-, (C) GFP-CDC-42-, or (D) GFP-RHO-1-expressing embryos were partially depleted of DYN-1 by *dyn-1* fRNAi treatments, and the fluorescence intensities for GFP-PAR-6, percentage of cortical area occupied for GFP-PAR-2, or the percentage of cortical area of foci for GFP-CDC-42 and GFP-RHO-1 within the anterior and posterior halves were quantified. Results are the mean ± SD from more than six independent experiments. For GFP-PAR-6 and GFP-PAR-2, fluorescence intensities or percentage of cortical area were quantified at the time of pseudocleavage formation (E, establishment phase) and pronuclear rotation (M, maintenance phase). For GFP-CDC-42 and GFP-RHO-1, the time of pseudocleavage (E) and pronuclear meeting (M) were chosen for quantification. (E) Comparison of ratio of asymmetry (see Experimental Procedures) between WT and *dyn-1* fRNAi-treated GFP-PAR-6, GFP-PAR-2, GFP-CDC-42, and GFP-RHO-1 embryos during establishment (E) and maintenance (M) phases. Results are the mean ± SD from more than six independent experiments. In all graphs, asterisks indicate level of significance for compared data as follows: $^{*}p < 0.05$; $^{**}p < 0.01$; $^{***}p < 0.001$. Scale bars, 10 μm.

We examined whether the anterior localization of DYN-1 was dependent upon the anterior PAR proteins by depleting PAR-6 or PKC-3. In *par-6* or *pkc-3* fRNAi-treated embryos, DYN-1b^{FL}-GFP became evenly distributed throughout the cortex during the maintenance phase (Figure 1D; *par-6* fRNAi, n = 12; *pkc-3* fRNAi, n = 6). Since PAR-6 and PKC-3 are necessary for the establishment of polarity (Munro et al., 2004), these data suggest that localization of DYN-1 foci to the anterior cortex is regulated by anterior polarity cues.

DYN-1 Maintains PAR-6 in the Anterior Cortex

Polarity is established by the time of pseudocleavage formation and maintained through pronuclear rotation (Munro et al., 2004). To determine the role of DYN-1 during this time, the fluorescence intensities of GFP-PAR-6 within the anterior and posterior half were quantified at pseudocleavage formation (establishment phase) and at pronuclear rotation (maintenance phase). In WT embryos, fluorescence intensities in the anterior were significantly greater than those in the posterior at the end of the establishment phase. This intensity differential was retained through the maintenance phase (Figure 2A). A majority of the *dyn-1* fRNAi-treated embryos formed a normal GFP-PAR-6 cortical domain during the establishment phase (n = 7/9); however, GFP-PAR-6 levels were significantly lower at the anterior cortex during the maintenance phase (n = 5/7) (p = 0.01249; WT, n = 10; *dyn-1* fRNAi, n = 9) (Figures 2A and 2E), suggesting that DYN-1 is involved in maintaining the anterior localization of PAR-6.

DYN-1 Depletion Leads to Altered PAR-2 Localization

One of the posterior PAR proteins, PAR-2 (Boyd et al., 1996), is not required for the establishment of polarity, but is crucial for maintaining anterior PARs and the actomyosin network in the anterior cortex (Cuenca et al., 2003; Munro et al., 2004). Since DYN-1 depleted embryos failed to maintain PAR-6 in the anterior cortex, we next examined the effects of *dyn-1* fRNAi treatment on GFP-PAR-2 localization at the same time points as for GFP-PAR-6. In WT embryos, the posterior cortex was entirely labeled with GFP-PAR-2, and this localization was retained through the maintenance phase. In *dyn-1* fRNAi-treated embryos, GFP-PAR-2 labeled the posterior cortex at the establishment phase, similar to WT embryos (Figure 2B). However, at the maintenance

phase, the area occupied by GFP-PAR-2 expanded into the anterior (Figure 2B), resulting in a significant change in the cortical area occupied by GFP-PAR-2 (Figure 2E; p = 0.0059; WT, n = 6; *dyn-1*, n = 11). These data suggest that, in the absence of DYN-1, PAR-2 loses its proper posterior localization, likely as a result of the failure to maintain PAR-6 properly in the anterior cortex (Figure 2A), which has been described previously (Watts et al., 1996).

CDC-42 and RHO-1 Are Restricted to the Anterior Cortex by DYN-1

Since partial DYN-1 depletion leads to the failure of PAR-6 maintenance (Figure 2A), as well as defects in spindle pole movement similar to those reported for *cdc-42* RNAi-treated embryos (Motegi and Sugimoto, 2006), we sought to determine if CDC-42 was also misregulated. In WT embryos, the cortical area of GFP-CDC-42 foci is established and maintained at a relatively constant level at the anterior until pronuclear rotation (n = 8; Figure 2C). In *dyn-1* fRNAi-treated embryos, we observed GFP-CDC-42 foci localization to the anterior half of the embryo during the establishment phase (Figure 2C). However, during the maintenance phase, the cortical foci expanded into the posterior cortex (Figure 2C). A significant decrease in the ratio of anterior cortical area to the total cortical area of GFP-CDC-42 foci occurred at the maintenance phase (Figures 2E; p = 0.00026; WT, n = 8; *dyn-1* fRNAi, n = 8), similar to our quantification of GFP-PAR-2. These data suggest that DYN-1 is required for the continued restriction of CDC-42 foci to the anterior cortex during the maintenance phase.

RHO-1 is a small GTPase that regulates the polarization of Cdc42 and the actin cytoskeleton (Hall, 1998), which is responsible for the cortical flows that direct PAR-6, PAR-3, and PKC-3 to the anterior during the establishment phase (Schonegg and Hyman, 2006). Thus far, a role for RHO-1 during the maintenance phase has not been reported, since depletion of RHO-1 leads to disruption of polarity establishment (Schonegg and Hyman, 2006). To explore the role of DYN-1 in RHO-1 distribution during the maintenance phase, we examined *dyn-1* fRNAi-treated embryos expressing GFP-RHO-1 and quantified the area occupied by GFP-RHO-1 foci at the cortex (Figure 2D). We found that GFP-RHO-1 signal at the anterior cortex became significantly reduced during the maintenance phase (Figure 2D; p = 0.00044 [n = 9]; WT, n = 8; *dyn-1* fRNAi, n = 9). These data suggest that DYN-1 is required for the maintenance of RHO-1 specifically during the maintenance phase.

Dynamics of PAR-6 Partly Depend on DYN-1 during the Maintenance Phase

PAR-6 dynamically associates with the cortex during the cortical flow responsible for establishing PAR asymmetry (Cheeks et al., 2004). Since *dyn-1* fRNAi-treatment disrupted the anterior localization of GFP-PAR-6 during the maintenance phase, we suspected that the dynamics of PAR-6 change at the transition from polarity establishment to the maintenance phase. To address this, we photobleached a selected region of GFP-PAR-6 associated with the cortex in embryos, and monitored fluorescence recovery after photobleaching (FRAP). The photobleached region of the cortex quickly recovered fluorescence and reached a plateau around 3 min (Figure 3). When the initial rates of FRAP were compared between the establishment (~5 min after the onset of cortical flow) and maintenance (pronuclear meeting) phases in WT embryos, the rate of recovery during the maintenance phase was slightly but significantly greater than that during the establishment phase (Figure 3B, left, right; p = 0.04836; establishment phase, n = 4; maintenance phase, n = 6), suggesting that the dynamics of PAR-6 are changed at the transition between these phases. The initial rate of FRAP during the maintenance phase was slightly decreased in *dyn-1* fRNAi-treated embryos, although the difference is not statistically significant (Figure 3B, middle, right; p = 0.101; WT, n = 6; dyn-1, n = 6). However, the levels of recovered fluorescence were decreased significantly in *dyn-1* fRNAi-treated embryos (Figure 3B, middle; p = 0.00852 at 5 min; WT, n = 6; dyn-1, n = 6), suggesting that the dynamics of GFP-PAR-6 partly depends on DYN-1 during the maintenance phase. These data also provide evidence that DYN-1-dependent dynamics of PAR-6 are responsible for the maintenance of polarity.

Dynamin-Dependent Actin Comet Formation Increases during the Maintenance Phase

The canonical role of dynamin is to regulate clathrin-dependent endocytosis (Hinshaw and Schmid, 1995; McNiven, 1998). DYN-1b^{FL}-GFP localized to the anterior cortex during the polarity maintenance phase, prompting us to examine whether endocytosis occurs at the anterior membrane during the maintenance phase. Since actin comets are hypothesized to be endocytic in nature (Fehrenbacher et al., 2003; Merrifield et al., 1999, 2001; Taunton, 2001; Taunton et al., 2000), we quantified the number of actin comets that formed during the polarity establishment and maintenance phases in embryos expressing a GFP-tagged fragment of moesin (GFP-moe) (Motegi et al., 2006). Only comets with an obvious tail that showed movement were counted. Similar to the pattern recently reported, the actomyosin network moved to the anterior with cortical flow and collapsed into smaller filaments, at which point actin comets began to form (Velarde et al., 2007) (Figure 4A). Interestingly, the generation of the majority of the actin comets was confined to the anterior region during the maintenance phase (10–18 min, n = 11) (Figure 4B). There was a significant decrease in the number of actin comets in *dyn-1* fRNAi-treated embryos during the early portion of the maintenance phase (Figure 4C, 10–13 min; p = 0.00038, Welch's t test; WT, n = 11; *dyn-1* fRNAi, n = 10). We did not, however, observe any obvious disruptions to the cortical actin network in the *dyn-1* fRNAi-treated embryos (data not shown). These data suggest a role for dynamin in regulating formation of the actin comets at the transition between the establishment and maintenance phases.

To further examine the possible link between actin comets and endocytosis, we stained embryos expressing GFP-RAB-5 with Alexa568-tagged phalloidin. The small GTPase, RAB-5, is one of the key regulators of early endocytic traffic (Semerdjieva et al., 2008; Zerial and McBride, 2001). We found RAB-5 very closely associated with many actin foci (Figure 4D). Interestingly, the shape of some of the actin foci (Figure 4D) was similar to that of the larger actin comets that we observed with GFP-moe (Figure 4A). We also discovered that the comet-like structures contained DYN-1b^{FL}-GFP (Figures 4E and 4F). In the live images, the DYN-1b^{FL}-GFP comets progressed through the cytoplasm

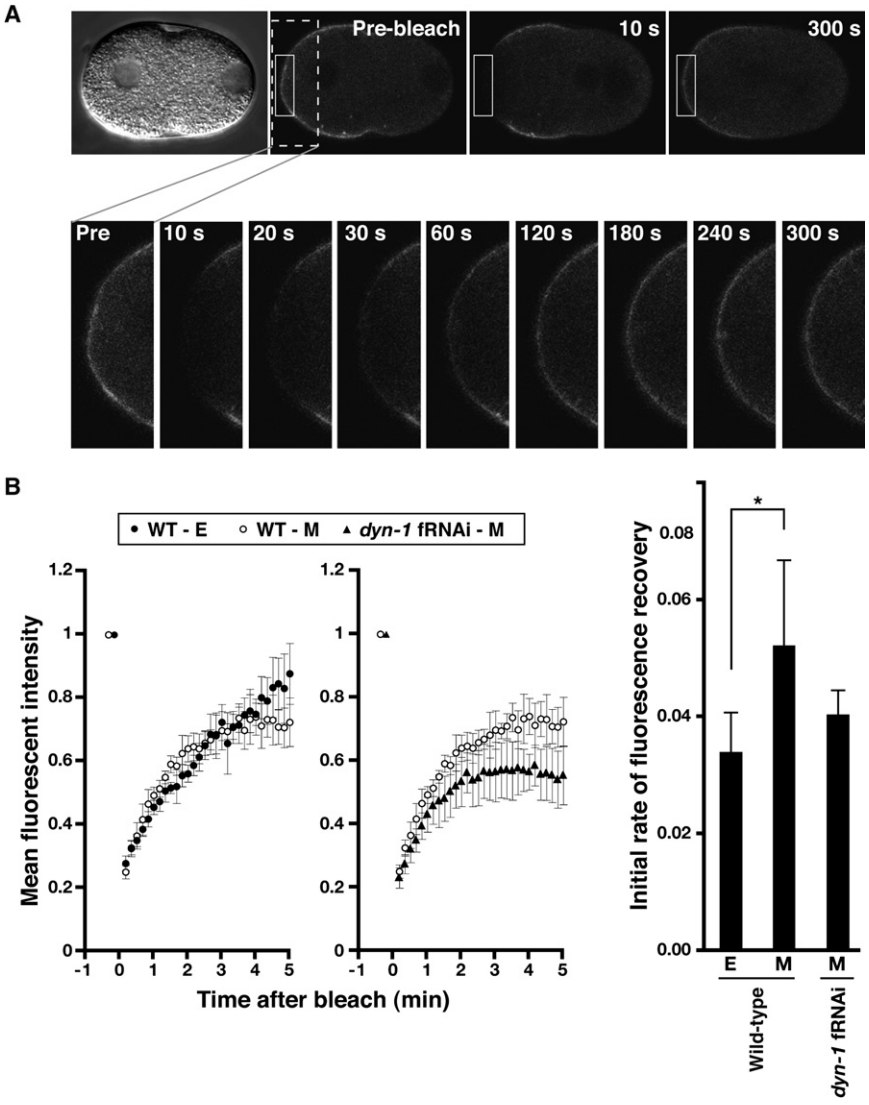

Figure 3. PAR-6 Dynamics Change between the Polarity Establishment and Maintenance Phases

(A) Photobleached embryo expressing GFP-PAR-6. At approximately pronuclear meeting, the anterior cortex was photobleached. DIC and fluorescent images just before photobleaching and at a designated time after photobleaching are shown. Solid line marks the photobleached area. Selected frames from the time-lapse recording around the bleached area are shown in the magnified images.

(B) (Left) The areas around the anterior cortex were photobleached at approximately 5 min after the onset of cortical flow (establishment phase) in WT or at the time just before pronuclear meeting (maintenance phase) in WT and *dyn-1* fRNAi-treated embryos (*dyn-1*). Images of the bleached area were taken every 10 s. Mean fluorescent intensity along the bleached cortex was measured and the ratios of mean fluorescent intensity after photobleaching to that before photobleaching are plotted. Time (min) is with respect to the bleach (time 0). Results are the mean ± SD from more than four independent experiments. E, establishment phase; M, maintenance phase; WT, wild-type. (Right) The initial recovery ratios of fluorescence along the bleached region are plotted. Results are the mean ± SD from more than four independent experiments. Differences between the establishment and maintenance phases in WT embryos are statistically significant. P value of M (n = 6) versus E (n = 4) is 0.048.

with a velocity of 0.2 μm/s, which is comparable to that reported for actin comets in mammalian cells (Orth et al., 2002).

Endocytosis from the Anterior Membrane Is Enriched during the Maintenance Phase

To directly visualize endocytic events, we used the fluorescent styryl dye, FM2-10 (Rizzoli and Betz, 2002), to examine bulk membrane dynamics in *C. elegans* embryos (Figure 5). Whereas, during pronuclear migration, numerous vesicles were observed near the anterior cortex, the posterior remained fairly free of vesicles (Figure 5A). During pronuclear centration/rotation (maintenance phase), a majority of the vesicle trafficking events originated from the anterior membrane and moved toward both spindle poles (Figure S4). We found that the number of vesicles endocytosed from the anterior was approximately three times more than that from the posterior (n = 4 embryos), and the ratio of vesicles endocytosed from the anterior to total number of vesicles was 0.74 ± 0.18 (n = 4). Interestingly, upon *dyn-1* fRNAi treatment, the observed enrichment of endocytic activity was lost and the ratio decreased significantly to 0.45 ± 0.20 (n = 6; p = 0.0424, Student's t test; Figure 5A). These results suggest that endocytosis occurs primarily at the anterior membrane during the maintenance phase, and that endocytosis in the anterior depends on DYN-1. Although the number of vesicles was decreased when embryos were treated with *dyn-1* fRNAi, we did not observe complete loss of endocytosis. This may result from either the presence of DYN-1-independent endocytosis or our partial depletion of DYN-1.

Because dynamin is required for scission of nascent endosomes from the plasma membrane, suppression of dynamin function can paradoxically reveal sites of active endocytosis by trapping invaginating membrane tubules at the plasma membrane, as shown in dynamin temperature-sensitive mutants (Kosaka and Ikeda, 1983; McNiven, 1998). We monitored plasma membrane dynamics at the mid-focal plane in *dyn-1* fRNAi-treated embryos expressing a fusion of GFP with a pleckstrin homology (PH) domain derived from mammalian PLC1δ1 (GFP-PH$^{PLC1\delta1}$) (Audhya et al., 2005; Hurley and Meyer, 2001). The *dyn-1* fRNAi-treated embryos displayed accumulations of what appeared to be vesicle-like structures at the anterior membrane, but not at the posterior membrane, during the maintenance phase (Figure 5B; n = ~10 vesicles for the anterior, ~4 vesicles for the posterior), further indicating that DYN-1-dependent endocytosis is enriched at the anterior membrane during the maintenance phase.

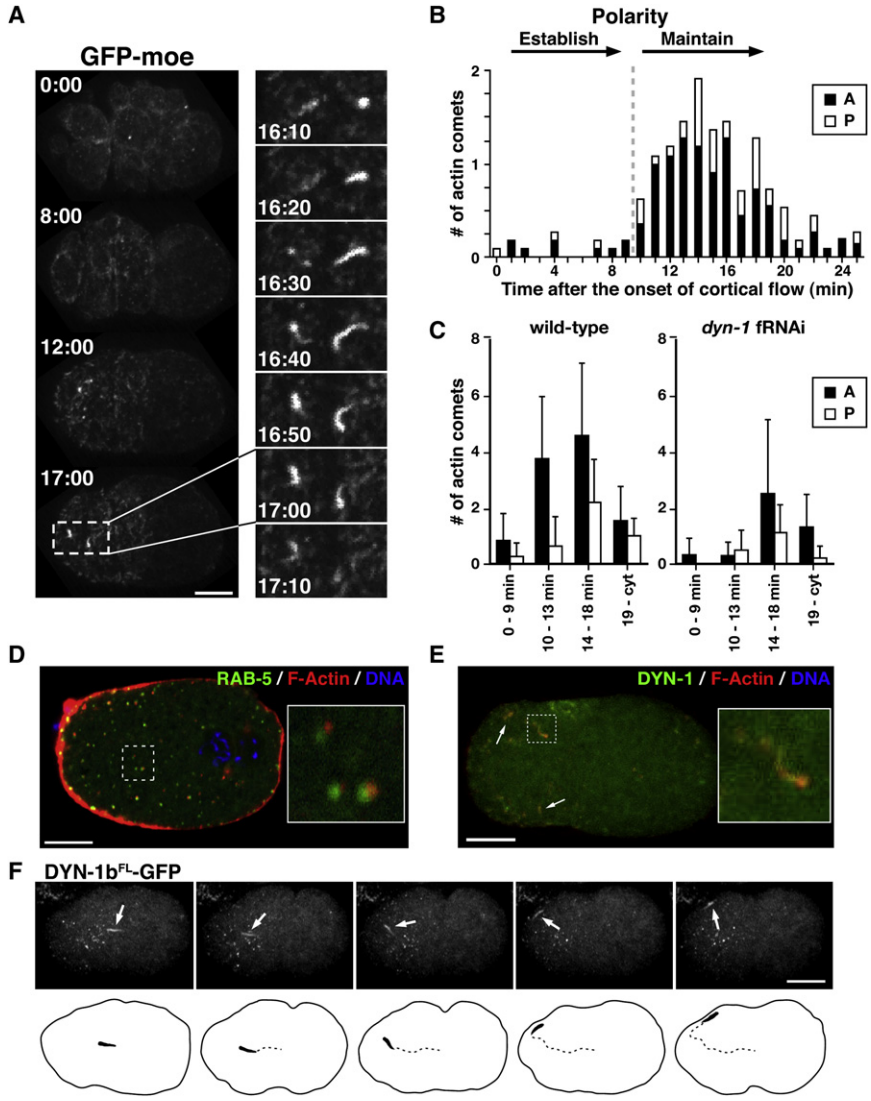

Figure 4. Dynamin-Dependent Actin Comet Dynamics Increase during the Maintenance Phase

(A) A series of images from a time-lapse recording of a GFP-moe-expressing embryo. Sequence images of boxed areas with dashed lines are magnified and aligned from top to bottom.

(B) The average numbers of actin comets per embryo at every minute are calculated from eleven independent embryos. A, anterior (closed bars); P, posterior (open bars). Times are with respect to the onset of cortical flow.

(C) Actin comets in WT and *dyn-1* fRNAi-treated embryos expressing GFP-moe were counted and the average number ± SD are plotted. P value of WT versus *dyn-1* fRNAi-treated embryos is 0.00038 (Welch's t test; WT, n = 11; *dyn-1*, n = 10).

(D) GFP-RAB-5-expressing embryos at pronuclear meeting were fixed and stained with Alexa568-conjugated phalloidin (red) and DAPI (blue). An image at mid-focal plane is shown, and an image in the boxed area (dashed line) is magnified (2.5×).

(E) DYN-1b^{FL}-GFP-expressing embryos at pronuclear meeting were fixed and stained with Alexa568-conjugated phalloidin (red). Z-series projection near the cortex is shown, and an image in the boxed area (dashed line) is magnified (2.5×). Arrows designate actin comets that are colocalized with DYN-1b^{FL}-GFP.

(F) A series of cortical images at 30 s intervals of a GFP-DYN-1b^{FL}-expressing embryo are shown. Arrows designate an individual actin comet-like structure with GFP fluorescence. Schematic depictions of the actin comet-like structure are shown below the images. Dashed lines show the trajectory of the movement. Scale bar, 10 μm.

PAR-6 Is Associated with Endocytic Markers in the Early Embryo

Since our data suggest that dynamin-regulated endocytosis at the anterior is required for polarity maintenance, we investigated whether PAR-6 associated with endocytic markers during the maintenance phase. Although PAR-6 vesicle-like structures rarely accumulate near the cortex in WT embryos (Figure 6A), numerous vesicle-like structures accumulated near the anterior membrane in *dyn-1* fRNAi-treated embryos during the maintenance phase. These PAR-6-labeled puncta could be associated with invaginated membrane that is unable to be pinched off. Additionally, PAR-6 is not observed as endomembrane (Figure 6A), suggesting that vesicle-like puncta associated with PAR-6 might be rapidly recycled back to the anterior cortex and difficult to detect in WT embryos. To determine if DYN-1 was involved in the formation of the PAR-6-labeled intracellular puncta, we imaged a strain expressing both DYN-1-GFP and mCherry-PAR-6. We often detected mCherry-PAR-6-labeled puncta emerging at or near sites of DYN-1-GFP foci in the anterior cortex during the maintenance phase (Figure 6B; establishment phase embryo shown in Figure S5). Quantification revealed that 73% ± 14% of the PAR-6 puncta release sites were also sites of DYN-1-GFP foci accumulation just prior to PAR-6 internalization (n = 11 embryos). The intensity of DYN-1-GFP foci at the PAR-6 emergence sites diminished over time as the PAR-6 puncta were internalized, suggesting that DYN-1 may function early in the process of PAR-6 internalization.

Next, we determined that some of the GFP-PAR-6 puncta were closely associated with endocytosed FM1-43 dye in *dyn-1* fRNAi-treated embryos (Figure 6C). Given all of the data that we have observed, the results presented in Figure 6 suggest that the PAR-6 puncta may be endocytic. We examined fixed embryos stained for different endocytic and trafficking markers to determine if PAR-6 was trafficked through endocytic compartments. The vesicle-regulating protein, RAB-5, was partially localized at the PAR-6-labeled anterior cortex in WT embryos (Figure S6A). EEA-1, a marker for the early endosomes, also partially overlapped with PAR-6 accumulations at the cortex (Figure S6B). PAR-6 was not obviously associated with RAB-11, a recycling endosome marker, during the maintenance phase (Figure S6C). While the overlap that we observed for RAB-5 and EEA-1 was partial in nature, these data are suggestive of a potential mechanism in which PAR-6 could be rapidly recycled back to the anterior cortex.

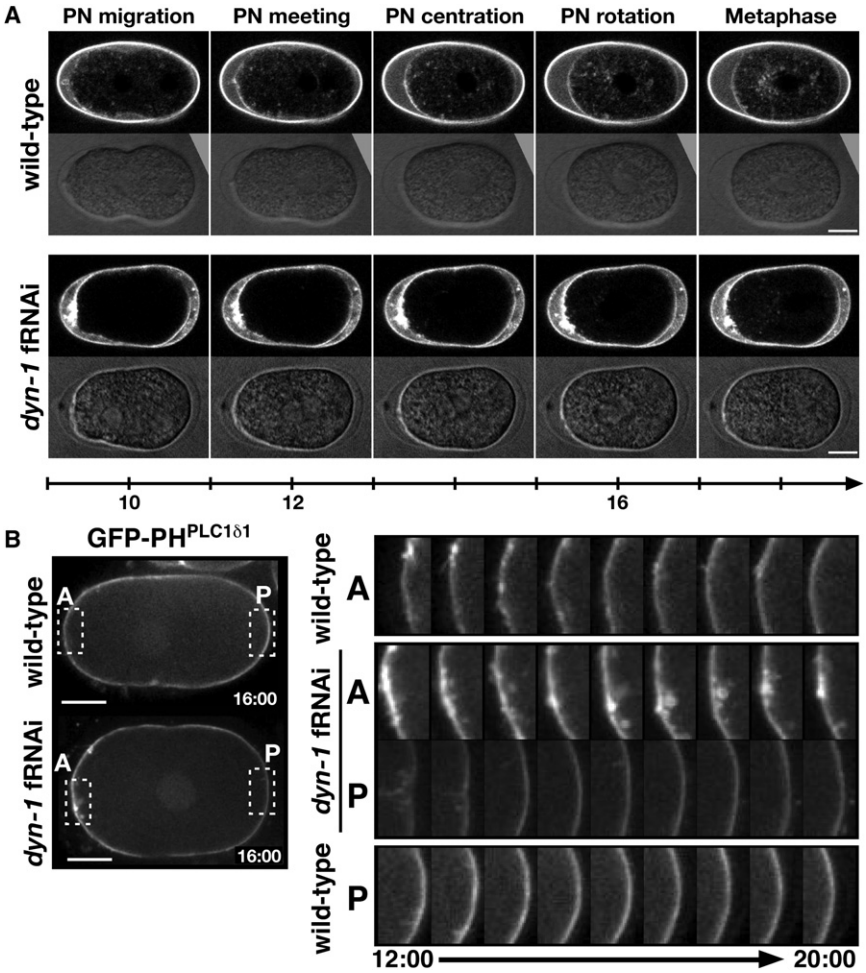

Figure 5. Endocytosis at the Anterior Cortex Is Enriched during the Maintenance Phase

(A) Time-lapse images from WT and *dyn-1* fRNAi-treated embryos were labeled with the fluorescent membrane dye, FM2-10, and imaged using multi-photon microscopy. Transmitted light panels show the cell cycle phase.

(B) Time-lapse recordings at the mid focal plane in WT or *dyn-1* fRNAi-treated embryos expressing $PH^{PLC1\delta1}$-GFP. Images from time-lapse recordings at 16:00 min are shown. A series of images during the maintenance phase (12:00–20:00) of the boxed area (dashed line) are shown magnified. Time (min) is with respect to the onset of cortical flow. A, anterior; P, posterior. Scale bars, 10 μm.

DISCUSSION

In the present study, we found that dynamin (DYN-1) plays a central role in the maintenance of anterior embryonic polarity by maintaining the anterior polarity factors in the developing *C. elegans* embryo. DYN-1-GFP foci are enriched in the anterior cortex and maintained there by PAR-6 and PKC-3. Endocytosis becomes enriched in the anterior during the polarity maintenance phase, but is hindered in *dyn-1* fRNAi-treated embryos, and these embryos subsequently fail to maintain the previously established PAR asymmetry. These results demonstrate a mechanism for the spatial and temporal regulation of endocytosis in the anterior of the embryo, contributing to the precise localization and maintenance of polarity factors within a dynamic plasma membrane.

Results from the FRAP and FM2-10 dye uptake experiments suggest that DYN-1 may be responsible for the observed change in membrane dynamics specifically during the maintenance phase. Recent work identified the anterior polarity factors, PAR-6, PAR-3, PKC-3, and CDC-42, as regulators of endocytosis (Balklava et al., 2007). Given that dynamin can regulate both endocytic and actin dynamics in animal cells, and that actin regulators play a central role in endocytosis (Kaksonen et al., 2006; Merrifield, 2004; Merrifield et al., 2002, 2005; Smythe and Ayscough, 2006), we suggest that dynamin could also maintain anterior polarity by regulating endocytic actin dynamics.

Before polarity is established, DYN-1 is distributed throughout the embryo cortex. However, our FM2-10 experiments suggest that the observed increase in endocytic activity from the anterior does not occur until DYN-1 is enriched in the anterior and the maintenance phase begins. Cortical localization of PAR-6 requires CDC-42 for the maintenance of polarity, but not establishment (Aceto et al., 2006), suggesting that the CDC-42/PAR-6 complex may form during the maintenance phase. Furthermore, these findings raise the possibility that the formation of the larger CDC-42/PAR-6/PAR-3/PKC-3 complex during the maintenance phase may be required to stimulate endocytosis. Recently, Cdc42 and the PAR complex were found to play a key role in stabilizing adherens junctions through regulation of endocytosis at the apical membrane (Harris and Tepass, 2008). In mammals, Cdc42 increases the activity of aPKC by regulating Par6 (Atwood et al., 2007), and it is possible that this interaction activates endocytosis (Nishimura and Kaibuchi, 2007).

PIP_2 membranes, labeled by GFP-$PH^{PLC1\delta1}$, are also anteriorly localized in a PAR-6-dependent manner during the maintenance phase (see Supplemental Data and Figure S7). Given that endocytosis often occurs from PIP_2-rich membranes (Chung et al., 1997), accumulation of PIP_2 may act as the trigger of endocytosis in the anterior. Additionally, PIP_2 can recruit dynamin to the cortex in mammalian cells (Salim et al., 1996). Taken together, it is likely that cortical flow may transport the endocytic machinery and signaling molecules to the anterior, where they act to maintain the established polarity (Munro et al., 2004) through endocytosis. The recruitment of DYN-1 foci to the anterior might also be regulated by anteriorly localized PIP_2. Our data suggest a feedback loop mechanism necessary for the maintenance of anterior PAR asymmetry (Figure 7).

Protein accumulation within a fluid and dynamic membrane could be maintained by membrane recycling. Mathematical

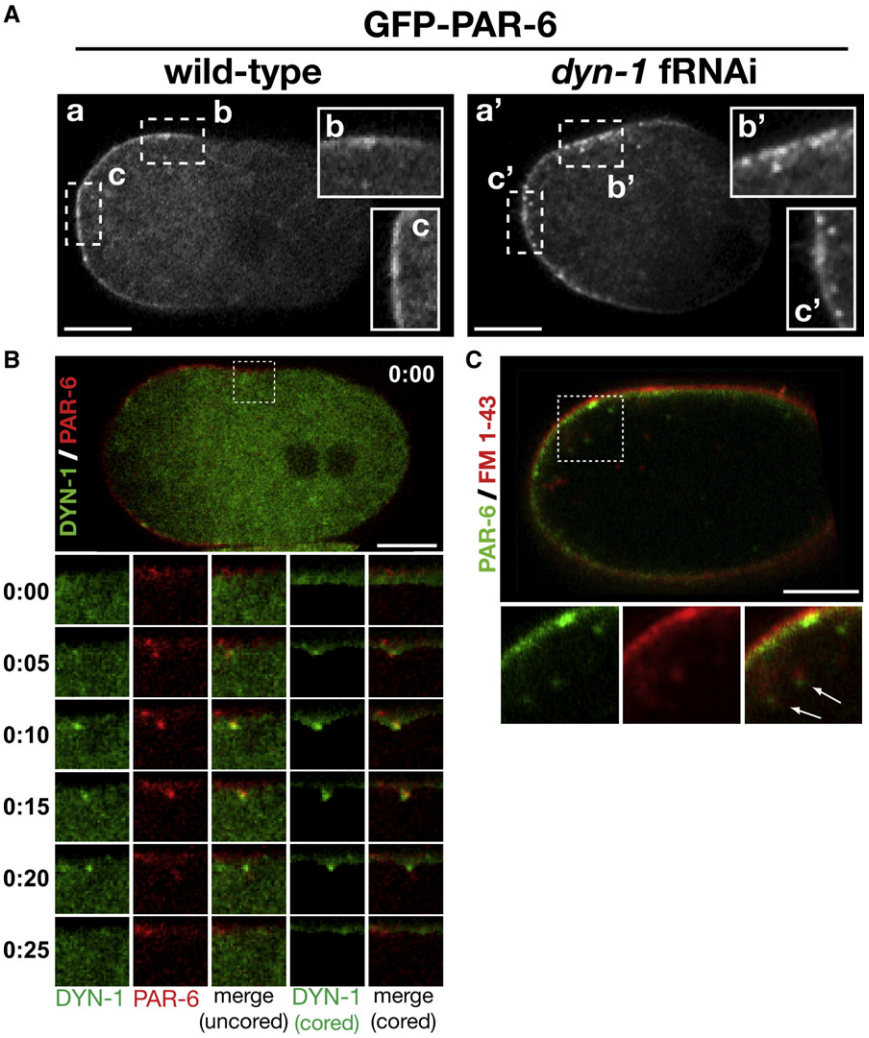

Figure 6. PAR-6 Is Closely Associated with Endocytic Markers

(A) Images of WT and *dyn-1* fRNAi-treated embryos expressing GFP-PAR-6 at pronuclear rotation. Insets show magnified view of regions in dashed boxes.

(B) Image of WT embryo expressing DYN-1-GFP and mCherry-PAR-6 during the maintenance phase (pronuclear [PN] meeting). Below, zoomed-in time series of the boxed region of the whole embryo in individual and merged channels. From left: uncored DYN-1-GFP; mCherry-PAR-6; merge of uncored DYN-1-GFP and mCherry-PAR-6; cored DYN-1-GFP (see Experimental Procedures); and merge of cored DYN-1-GFP and mCherry-PAR-6. Time 0:00 is the point at which the PAR-6 punctum can first be observed emerging. Images were taken every 5 s. Scale bar, 10 μm.

(C) GFP-PAR-6-expressing embryos were treated with *dyn-1* fRNAi and labeled with FM1-43 membrane dye. Embryo shown is in early maintenance phase (late PN migration). Arrows in zoomed image indicate examples of colocalized or partially overlapped GFP-PAR-6 foci and FM1-43-labeled vesicles. Scale bar, 10 μm.

models have predicted that endocytosis and recycling would provide the optimal conditions to limit a protein to a distinct membrane domain (Marco et al., 2007). Our data show an association of PAR-6 puncta with DYN-1-GFP foci, and a partial association with FM dye and other endocytic markers (Figure 6 and Figure S6) during the maintenance phase, suggesting that an endocytic mechanism may function to maintain PAR-6 localization to the anterior. Due to the dynamic nature of the trafficking process, the fluidity of the plasma membrane itself, and the multiple cellular compartments potentially involved in maintaining membrane domains, PAR-6 was not expected to be entirely within the early endocytic compartments at one given time, as we have observed. Instead, we propose that selective, fast recycling of cortical proteins could contribute to the formation of a distinct anterior membrane domain.

PAR-6 is thought to bind to the cortex partly through a direct interaction with CDC-42 (Aceto et al., 2006; Gotta et al., 2001). In addition to the reduced PAR-6 levels at the cortex, CDC-42 spreads into the posterior cortex in *dyn-1* fRNAi-treated embryos (Figure 2C), raising the possibility that dynamin-regulated endocytosis may prevent anteriorly localized polarity cues from diffusing laterally beyond the anterior cortical domain. The spread of anteriorly accumulated CDC-42 to the posterior may decrease CDC-42 levels such that PAR-6 can no longer bind to the cortex within both the anterior and the posterior domains. Given this, we suggest that endocytosis and recycling of PAR-6, and possibly CDC-42, to the anterior cortex may be responsible for the maintenance of PAR-6 to the anterior cortex.

Actin comets have been observed in several different systems, and it is hypothesized that they are actin-based endocytic events (Fehrenbacher et al., 2003; Lee and De Camilli, 2002; Merrifield et al., 1999, 2001; Orth et al., 2002; Taunton, 2001; Taunton et al., 2000). Additionally, recent work has revealed that dynamin, Arp2/3, and Cdc42 function together to regulate actin-mediated endocytosis and, subsequently, adherens junction maintenance and E-cadherin localization in epithelial tissues (Georgiou et al., 2008; Leibfried et al., 2008), suggesting that actin-associated endocytosis could be a common maintenance mechanism in polarized cells. We cannot rule out the possibility that *dyn-1* fRNAi treatment causes subtle perturbations in the actin cytoskeleton that we are unable to detect, and that this also contributes to polarity disruption. However, this mechanism is not necessarily exclusive of the mechanism that we propose—that endocytosis regulates polarity maintenance. We found that the formation of actin comets is consistent with the timing of an increase in endocytosis from the anterior membrane, and *dyn-1* fRNAi treatment affects both endocytosis and actin comet formation. RAB-5-labeled puncta are also closely associated with actin foci, further suggesting that they are endocytic in nature. Given all of our data, the formation of actin comets at this precise point in development likely reflects endocytosis.

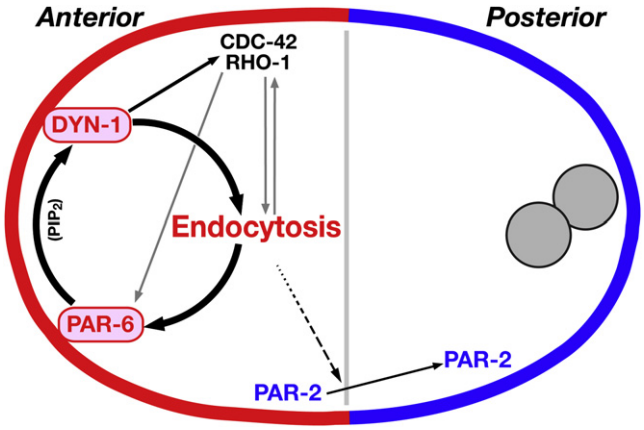

Figure 7. Model

PAR-6 appears to be at the top of a regulatory cascade involved in maintaining polarity cues in the anterior of the embryo, based on our observations (bold black arrows) and including those of others (gray arrows). During the polarity maintenance phase, PAR-6 functions to maintain DYN-1 foci to the anterior, possibly through regulating anterior accumulation of PIP_2. DYN-1 regulates endocytic events from the anterior cortex and regulates anterior accumulation of PAR-6. DYN-1 also regulates accumulation of CDC-42 and RHO-1 to the anterior. It has been reported that CDC-42 regulates anterior association of PAR-6 and endocytosis. We also propose that endocytosis removes PAR-2 from the anterior cortex and transports it to the posterior cortex (arrow with broken line).

Previous work has shown that loss of anterior polarity cues leads to an expansion of the posterior PARs into the anterior cortex (Boyd et al., 1996; Kay and Hunter, 2001; Watts et al., 1996). PAR-2 expansion into the anterior half of the embryo was observed in a majority of the *dyn-1* fRNAi-treated embryos, suggesting that DYN-1 might normally play an active role in removing PAR-2 from the anterior cortex. Here, an endocytic mechanism could exist in which posterior polarity cues are actively being removed from the anterior membrane throughout development. In meiosis, PAR-2 is normally localized in a small cortical area in the anterior surrounding the polar body, although PAR-2 is rapidly removed from the anterior cortex soon after (Boyd et al., 1996; Cuenca et al., 2003). In *dyn-1* RNAi-treated embryos, the anterior cap of PAR-2 is absent (Figure 2B). This suggests that DYN-1 may mediate the maintenance of PAR-2 near the polar body. The function of PAR-2 in the polar body or in meiosis remains unclear, but it seems possible that DYN-1 plays a key role in maintaining polarized membrane domains during development.

In conclusion, our data suggest that a mechanism exists in which dynamin plays a key role in maintaining polarity within defined regions of the plasma membrane in the early embryo. Here, an enrichment of endocytic machinery, coupled with actin cytoskeleton remodeling machinery, is maintained in a spatial and temporal manner with respect to polarity cues. Further analysis will be required to determine which factors are recycled and what cues are used to target these factors back to specific membrane sites. Ultimately, answering these questions will help define the mechanisms required to maintain polarity within a fluid and dynamic plasma membrane throughout development.

EXPERIMENTAL PROCEDURES

RNA Interference

For the *dyn-1* fRNAi experiments, the *dyn-1* gene was obtained from the Ahringer RNAi feeding library (Kamath and Ahringer, 2003). Knockdown of gene function was performed using RNA interference feeding methods (Kamath et al., 2003). The temperature for fRNAi treatments was the same as that used for maintenance of the specific worm strains. Complete depletion of DYN-1 results in decreased brood size, embryonic lethality, and sterility due to defects in embryogenesis and incomplete cellularization of the syncytial gonad (Thompson et al., 2002). Therefore, we used conditions that only partially deplete DYN-1. Bacterial cultures containing the *dyn-1* feeding RNAi vector were diluted with bacterial cultures containing the L4440 vector alone (1:3–1:5) to weaken the RNAi effect. Using these diluted cultures and feeding times of only 18–24 hr allowed production of normal-shaped embryos. At 25°C after 24 hr of *dyn-1* feeding, 74% fewer embryos were produced, and the embryonic lethality within these embryos was 13% (data not shown).

Live Imaging and Analysis of GFP Fluorescence

GFP time-lapse video images were captured using a motorized microscope (Axlovert 200M; Zeiss) equipped with a spinning disc confocal scan head (QLC100; Visitech International). For additional details, see Supplemental Data.

Kymograph Analysis

For analyses of GFP-fusion movement, kymographs were made with ImageJ software. Cortical time-lapse recordings of appropriate strains were obtained at 10–15 s intervals. Subregions on a straight line along the long axis of the embryo were extracted from each image and stacked vertically into single kymograph images.

Fluorescence Intensity Analysis

To analyze *dyn-1* fRNAi effects on GFP-PAR-6 distribution, the cortical area of the embryo on the time-lapse recording was divided into two anterior and posterior halves of approximately equal cortical areas. The fluorescence intensity in each area was measured with ImageJ at the establishment (pseudocleavage) and maintenance phases (pronuclear meeting or centration), and background fluorescence intensity obtained from a WT, non-GFP-expressing embryo was subtracted. The distribution of GFP-RHO-1 and GFP-CDC-42 foci was analyzed as described previously (Motegi and Sugimoto, 2006). Briefly, background fluorescent signals other than the major foci were removed by setting a threshold value that minimized background fluorescence in regions devoid of GFP foci. The areas of fluorescence above the threshold value in each anterior and posterior region were measured with the percent area measurement in the ImageJ measurement tools. The cortical area covered by GFP-PAR-2 was measured similarly to GFP-RHO-1 and GFP-CDC-42 (for more information, see Supplemental Data).

Vesicle Quantification

To quantify the number of vesicles observed in FM2-10-labeled embryos, vesicles were defined as fully formed puncta in which some separation from the membrane could be detected. Blebs or membrane tubulations, while likely to be endocytic events, were not counted unless vesicle release was detected. In ImageJ, boxes of approximately equal area were drawn at the anterior and posterior ends of the embryos. Vesicles originating from membrane within the boxes were counted. Due to variation in the efficiency of membrane labeling in FM2-10, ratios of anterior to total vesicles were determined for each individual experiment and averaged.

For analysis of DYN-1-GFP × mCherry-PAR-6, images were taken from pseudocleavage (~8:00 min) through mitosis. Using ImageJ, cytoplasmic signal from DYN-1-GFP was digitally cored only in the GFP channel prior to merging and counting the PAR-6-labeled intracellular puncta (Mohler et al., 1998). The rationale was that the cytoplasmic signal affected the detection of PAR-6 puncta internalization, and also that the PAR-6 puncta and DYN-1-GFP near the cortex were most relevant for this analysis. In counting the PAR-6 intracellular puncta, only puncta in which internalization from the cortex was detected were counted. The approximate site of internalization was then scored for DYN-1-GFP accumulation (in the form of foci) prior to and at the time the PAR-6 puncta emergence could be detected.

Statistical Analysis

To examine the effects of *dyn-1* fRNAi treatment, we quantified fluorescent intensities (for GFP-PAR-6) or cortical area of fluorescence (GFP-PAR-2, GFP-CDC-42, GFP-RHO-1) as described above. The quantified values within the anterior (GFP-PAR-6, GFP-CDC-42, GFP-RHO-1) or the posterior (GFP-PAR-2) were compared between WT and *dyn-1* fRNAi-treated embryos. For comparisons of the asymmetry, the ratio of the quantified value within the anterior to that within the whole embryo was calculated for embryos expressing GFP-PAR-6, GFP-CDC-42, or GFP-RHO-1. The ratio of the quantified value within the posterior to that within the whole embryo was calculated for embryos expressing GFP-PAR-2. The ratio was also compared between WT and *dyn-1* fRNAi-treated embryos. The F test was used to compare the variance between subjects before applying the t test. When the variance was equal, Student's t test (two tails) was used to analyze the difference between WT and *dyn-1* fRNAi-treated embryos. When the variances were unequal, Welch's t test was used. The statistical tests were done with the Statcel add-in program for Microsoft Excel (OMS Publishing, Tokorozawa, Japan). A p value of less than 0.05 was considered statistically significant.

FRAP

FRAP experiments were performed with a Zeiss LSM 510 laser scanning microscope with a 40×/1.3 NA EC Plan-NEOFLUAR oil-immersion objective. To accomplish photobleaching, the anterior cortex of interest was photobleached for 30 s at full laser power (100% laser). After photobleaching, the embryos were imaged every 10 s at low laser power (4% laser). Mean fluorescence intensities on the bleached cortex were quantified with ImageJ software.

FM Dye Imaging

For WT membrane dynamics, embryos were mounted on uncoated coverslips in hanging drops containing 100 μM FM2-10 (Molecular Probes) in egg buffer. The egg shell was ablated with a nitrogen-pumped coumarin 450 dye laser (Laser Sciences) to permit ingression of the label, as previously described (Skop et al., 2001; Squirrell et al., 2006). Simultaneous fluorescence (890 nm, two-photon excitation) and bright-field images were recorded every 4.4 s on a multiphoton, laser-scanning microscope, which is part of an optical workstation (White et al., 2001; Wokosin et al., 2003), with a Nikon 100X S Fluor (1.3 NA) lens. Due to possible egg shell defects in *dyn-1* fRNAi-treated embryos, for the *dyn-1* RNAi membrane dynamic comparison all embryos were mounted as above in membrane dye while the egg shell was still permeable, as control embryos can incorporate the membrane dye early in the cell cycle, prior to completion of egg shell formation (Bembenek et al., 2007). N2 worms were fed bacteria expressing either L4440 vector or *dyn-1* fRNAi (1:5 dilution, 20–26 hr).

Embryos expressing GFP-PAR-6 were treated with 1:5 diluted *dyn-1* fRNAi and mounted on uncoated coverslips in hanging drops containing 1 μg/ml FM1-43 (Molecular Probes) in egg buffer, as described above. Simultaneous fluorescence (890 nm, two-photon excitation) and bright-field images were recorded every 1.3–2 s on a multiphoton laser scanning microscope using a Nikon 60× Plan Apo VC (1.40 NA) lens. Fluorescence emissions were separated in alternating scans with a manual filter slider containing a 520/35 nm filter (for GFP) and a 580 nm long-pass filter (for FM1-43). To generate merged images, scans were deinterleaved in ImageJ into separate channels and subsequently merged and postprocessed in Adobe Photoshop CS.

SUPPLEMENTAL DATA

Supplemental Data include Supplemental Experimental Procedures and seven figures, and thirty-five movie files corresponding to the images presented in the figures and can be found with this article online at http://www.cell.com/developmental-cell/supplemental/S1534-5807(09)00171-3.

ACKNOWLEDGMENTS

Ahna R. Skop would like to dedicate this paper to her dear father, Michael Roe Skop, who passed away on May 31, 2009. We thank J.G. White, A. Ikeda, M. Otegui, K. Verbrugghe, W. Bement, P. Anderson, and R.D. White for suggestions and comments on the manuscript, and K. Kemphues, B. Bowerman, K. Oegema, G. Seydoux, J.G. White, A.M. van der Bliek, A. Hyman, and E. Munro for their generous gifts of reagents or advice. We thank Y. Kang and M. Li for assistance. Some of the worm strains used in this study were kindly provided by the *Caenorhabditis* Genetics Center, which is funded by the National Institutes of Health National Center for Research Resources. This work was supported by startup funds from the University of Wisconsin-Madison (to A.R.S), K01 Early Career Award HL092583-01 (to A.R.S), and grants-in-aid for scientific research from the Japanese Ministry of Education, Culture, Sports, Science, and Technology (to Y.N.). Y.N. and J.M.S. designed and performed the majority of the experiments, data analysis, and equally contributed to this work. D.S.P., J.M.Squirrell, J.M.K., J.B.S., and A.R.S. contributed data, expertise, and assisted with the manuscript. A.R.S. was responsible for project guidance.

Received: April 6, 2008
Revised: March 24, 2009
Accepted: April 21, 2009
Published: June 15, 2009

REFERENCES

Aceto, D., Beers, M., and Kemphues, K.J. (2006). Interaction of PAR-6 with CDC-42 is required for maintenance but not establishment of PAR asymmetry in *C. elegans*. Dev. Biol. *299*, 386–397.

Albertson, D.G. (1984). Formation of the first cleavage spindle in nematode embryos. Dev. Biol. *101*, 61–72.

Altschuler, Y., Barbas, S.M., Terlecky, L.J., Tang, K., Hardy, S., Mostov, K.E., and Schmid, S.L. (1998). Redundant and distinct functions for dynamin-1 and dynamin-2 isoforms. J. Cell Biol. *143*, 1871–1881.

Altschuler, Y., Liu, S., Katz, L., Tang, K., Hardy, S., Brodsky, F., Apodaca, G., and Mostov, K. (1999). ADP-ribosylation factor 6 and endocytosis at the apical surface of Madin-Darby canine kidney cells. J. Cell Biol. *147*, 7–12.

Andrews, R., and Ahringer, J. (2007). Asymmetry of early endosome distribution in *C. elegans* embryos. PLoS ONE *2*, e493. 10.1371/journal.pone.0000493.

Atwood, S.X., Chabu, C., Penkert, R.R., Doe, C.Q., and Prehoda, K.E. (2007). Cdc42 acts downstream of Bazooka to regulate neuroblast polarity through Par-6 aPKC. J. Cell Sci. *120*, 3200–3206.

Audhya, A., Hyndman, F., McLeod, I.X., Maddox, A.S., Yates, J.R., 3rd, Desai, A., and Oegema, K. (2005). A complex containing the Sm protein CAR-1 and the RNA helicase CGH-1 is required for embryonic cytokinesis in *Caenorhabditis elegans*. J. Cell Biol. *171*, 267–279.

Balklava, Z., Pant, S., Fares, H., and Grant, B.D. (2007). Genome-wide analysis identifies a general requirement for polarity proteins in endocytic traffic. Nat. Cell Biol. *9*, 1066–1073.

Bejsovec, A., and Wieschaus, E. (1995). Signaling activities of the *Drosophila* wingless gene are separately mutable and appear to be transduced at the cell surface. Genetics *139*, 309–320.

Bembenek, J.N., Richie, C.T., Squirrell, J.M., Campbell, J.M., Eliceiri, K.W., Poteryaev, D., Spang, A., Golden, A., and White, J.G. (2007). Cortical granule exocytosis in *C. elegans* is regulated by cell cycle components including separase. Development *134*, 3837–3848.

Boyd, L., Guo, S., Levitan, D., Stinchcomb, D.T., and Kemphues, K.J. (1996). PAR-2 is asymmetrically distributed and promotes association of P granules and PAR-1 with the cortex in *C. elegans* embryos. Development *122*, 3075–3084.

Chabu, C., and Doe, C.Q. (2008). Dap160/intersectin binds and activates aPKC to regulate cell polarity and cell cycle progression. Development *135*, 2739–2746.

Cheeks, R.J., Canman, J.C., Gabriel, W.N., Meyer, N., Strome, S., and Goldstein, B. (2004). *C. elegans* PAR proteins function by mobilizing and stabilizing asymmetrically localized protein complexes. Curr. Biol. *14*, 851–862.

Chung, J.K., Sekiya, F., Kang, H.S., Lee, C., Han, J.S., Kim, S.R., Bae, Y.S., Morris, A.J., and Rhee, S.G. (1997). Synaptojanin inhibition of phospholipase D activity by hydrolysis of phosphatidylinositol 4,5-bisphosphate. J. Biol. Chem. *272*, 15980–15985.

Cowan, C.R., and Hyman, A.A. (2007). Acto-myosin reorganization and PAR polarity in *C. elegans*. Development *134*, 1035–1043.

Cuenca, A.A., Schetter, A., Aceto, D., Kemphues, K., and Seydoux, G. (2003). Polarization of the *C. elegans* zygote proceeds via distinct establishment and maintenance phases. Development *130*, 1255–1265.

Deborde, S., Perret, E., Gravotta, D., Deora, A., Salvarezza, S., Schreiner, R., and Rodriguez-Boulan, E. (2008). Clathrin is a key regulator of basolateral polarity. Nature *452*, 719–723.

Emery, G., and Knoblich, J.A. (2006). Endosome dynamics during development. Curr. Opin. Cell Biol. *18*, 407–415.

Entchev, E.V., Schwabedissen, A., and Gonzalez-Gaitan, M. (2000). Gradient formation of the TGF-beta homolog Dpp. Cell *103*, 981–991.

Fehrenbacher, K., Huckaba, T., Yang, H.C., Boldogh, I., and Pon, L. (2003). Actin comet tails, endosomes and endosymbionts. J. Exp. Biol. *206*, 1977–1984.

Georgiou, M., Marinari, E., Burden, J., and Baum, B. (2008). Cdc42, Par6, and aPKC regulate Arp2/3-mediated endocytosis to control local adherens junction stability. Curr. Biol. *18*, 1631–1638.

Goldstein, B., and Macara, I.G. (2007). The par proteins: fundamental players in animal cell polarization. Dev. Cell *13*, 609–622.

Gotta, M., Abraham, M.C., and Ahringer, J. (2001). CDC-42 controls early cell polarity and spindle orientation in *C. elegans*. Curr. Biol. *11*, 482–488.

Grill, S.W., Gonczy, P., Stelzer, E.H., and Hyman, A.A. (2001). Polarity controls forces governing asymmetric spindle positioning in the *Caenorhabditis elegans* embryo. Nature *409*, 630–633.

Hall, A. (1998). Rho GTPases and the actin cytoskeleton. Science *279*, 509–514.

Harris, K.P., and Tepass, U. (2008). Cdc42 and Par proteins stabilize dynamic adherens junctions in the *Drosophila* neuroectoderm through regulation of apical endocytosis. J. Cell Biol. *183*, 1129–1143.

Hinshaw, J.E. (2000). Dynamin and its role in membrane fission. Annu. Rev. Cell Dev. Biol. *16*, 483–519.

Hinshaw, J.E., and Schmid, S.L. (1995). Dynamin self-assembles into rings suggesting a mechanism for coated vesicle budding. Nature *374*, 190–192.

Hird, S.N., and White, J.G. (1993). Cortical and cytoplasmic flow polarity in early embryonic cells of *Caenorhabditis elegans*. J. Cell Biol. *121*, 1343–1355.

Hurley, J.H., and Meyer, T. (2001). Subcellular targeting by membrane lipids. Curr. Opin. Cell Biol. *13*, 146–152.

Kaksonen, M., Toret, C.P., and Drubin, D.G. (2006). Harnessing actin dynamics for clathrin-mediated endocytosis. Nature reviews *7*, 404–414.

Kamath, R.S., and Ahringer, J. (2003). Genome-wide RNAi screening in *Caenorhabditis elegans*. Methods *30*, 313–321.

Kamath, R.S., Fraser, A.G., Dong, Y., Poulin, G., Durbin, R., Gotta, M., Kanapin, A., Le Bot, N., Moreno, S., Sohrmann, M., et al. (2003). Systematic functional analysis of the *Caenorhabditis elegans* genome using RNAi. Nature *421*, 231–237.

Kay, A.J., and Hunter, C.P. (2001). CDC-42 regulates PAR protein localization and function to control cellular and embryonic polarity in *C. elegans*. Curr. Biol. *11*, 474–481.

Kosaka, T., and Ikeda, K. (1983). Possible temperature-dependent blockage of synaptic vesicle recycling induced by a single gene mutation in *Drosophila*. J. Neurobiol. *14*, 207–225.

Lee, E., and De Camilli, P. (2002). Dynamin at actin tails. Proc. Natl. Acad. Sci. USA *99*, 161–166.

Leibfried, A., Fricke, R., Morgan, M.J., Bogdan, S., and Bellaiche, Y. (2008). *Drosophila* Cip4 and WASp define a branch of the Cdc42-Par6-aPKC pathway regulating E-cadherin endocytosis. Curr. Biol. *18*, 1639–1648.

Marco, E., Wedlich-Soldner, R., Li, R., Altschuler, S.J., and Wu, L.F. (2007). Endocytosis optimizes the dynamic localization of membrane proteins that regulate cortical polarity. Cell *129*, 411–422.

McNiven, M.A. (1998). Dynamin: a molecular motor with pinchase action. Cell *94*, 151–154.

Merrifield, C.J. (2004). Seeing is believing: imaging actin dynamics at single sites of endocytosis. Trends Cell Biol. *14*, 352–358.

Merrifield, C.J., Moss, S.E., Ballestrem, C., Imhof, B.A., Giese, G., Wunderlich, I., and Almers, W. (1999). Endocytic vesicles move at the tips of actin tails in cultured mast cells. Nat. Cell Biol. *1*, 72–74.

Merrifield, C.J., Rescher, U., Almers, W., Proust, J., Gerke, V., Sechi, A.S., and Moss, S.E. (2001). Annexin 2 has an essential role in actin-based macropinocytic rocketing. Curr. Biol. *11*, 1136–1141.

Merrifield, C.J., Feldman, M.E., Wan, L., and Almers, W. (2002). Imaging actin and dynamin recruitment during invagination of single clathrin-coated pits. Nat. Cell Biol. *4*, 691–698.

Merrifield, C.J., Perrais, D., and Zenisek, D. (2005). Coupling between clathrin-coated-pit invagination, cortactin recruitment, and membrane scission observed in live cells. Cell *121*, 593–606.

Mohler, W.A., Simske, J.S., Williams-Masson, E.M., Hardin, J.D., and White, J.G. (1998). Dynamics and ultrastructure of developmental cell fusions in the *Caenorhabditis elegans* hypodermis. Curr. Biol. *8*, 1087–1090.

Motegi, F., and Sugimoto, A. (2006). Sequential functioning of the ECT-2 RhoGEF, RHO-1 and CDC-42 establishes cell polarity in *Caenorhabditis elegans* embryos. Nat. Cell Biol. *8*, 978–985.

Motegi, F., Velarde, N.V., Piano, F., and Sugimoto, A. (2006). Two phases of astral microtubule activity during cytokinesis in *C. elegans* embryos. Dev. Cell *10*, 509–520.

Munro, E.M. (2006). PAR proteins and the cytoskeleton: a marriage of equals. Curr. Opin. Cell Biol. *18*, 86–94.

Munro, E., Nance, J., and Priess, J.R. (2004). Cortical flows powered by asymmetrical contraction transport PAR proteins to establish and maintain anterior-posterior polarity in the early *C. elegans* embryo. Dev. Cell *7*, 413–424.

Nishimura, T., and Kaibuchi, K. (2007). Numb controls integrin endocytosis for directional cell migration with aPKC and PAR-3. Dev. Cell *13*, 15–28.

Orth, J.D., and McNiven, M.A. (2003). Dynamin at the actin-membrane interface. Curr. Opin. Cell Biol. *15*, 31–39.

Orth, J.D., Krueger, E.W., Cao, H., and McNiven, M.A. (2002). The large GTPase dynamin regulates actin comet formation and movement in living cells. Proc. Natl. Acad. Sci. USA *99*, 167–172.

Rizzoli, S.O., and Betz, W.J. (2002). Effects of 2-(4-morpholinyl)-8-phenyl-4H-1-benzopyran-4-one on synaptic vesicle cycling at the frog neuromuscular junction. J. Neurosci. *22*, 10680–10689.

Salim, K., Bottomley, M.J., Querfurth, E., Zvelebil, M.J., Gout, I., Scaife, R., Margolis, R.L., Gigg, R., Smith, C.I., Driscoll, P.C., et al. (1996). Distinct specificity in the recognition of phosphoinositides by the pleckstrin homology domains of dynamin and Bruton's tyrosine kinase. EMBO J. *15*, 6241–6250.

Schafer, D.A. (2004). Regulating actin dynamics at membranes: a focus on dynamin. Traffic *5*, 463–469.

Schonegg, S., and Hyman, A.A. (2006). CDC-42 and RHO-1 coordinate acto-myosin contractility and PAR protein localization during polarity establishment in *C. elegans* embryos. Development *133*, 3507–3516.

Semerdjieva, S., Shortt, B., Maxwell, E., Singh, S., Fonarev, P., Hansen, J., Schiavo, G., Grant, B.D., and Smythe, E. (2008). Coordinated regulation of AP2 uncoating from clathrin-coated vesicles by rab5 and hRME-6. J. Cell Biol. *183*, 499–511.

Severson, A.F., and Bowerman, B. (2003). Myosin and the PAR proteins polarize microfilament-dependent forces that shape and position mitotic spindles in *Caenorhabditis elegans*. J. Cell Biol. *161*, 21–26.

Skop, A.R., Bergmann, D., Mohler, W.A., and White, J.G. (2001). Completion of cytokinesis in *C. elegans* requires a brefeldin A-sensitive membrane accumulation at the cleavage furrow apex. Curr. Biol. *11*, 735–746.

Smythe, E., and Ayscough, K.R. (2006). Actin regulation in endocytosis. J. Cell Sci. *119*, 4589–4598.

Squirrell, J.M., Eggers, Z.T., Luedke, N., Saari, B., Grimson, A., Lyons, G.E., Anderson, P., and White, J.G. (2006). CAR-1, a protein that localizes with the mRNA decapping component DCAP-1, is required for cytokinesis and

ER organization in *Caenorhabditis elegans* embryos. Mol. Biol. Cell *17*, 336–344.

Taunton, J. (2001). Actin filament nucleation by endosomes, lysosomes and secretory vesicles. Curr. Opin. Cell Biol. *13*, 85–91.

Taunton, J., Rowning, B.A., Coughlin, M.L., Wu, M., Moon, R.T., Mitchison, T.J., and Larabell, C.A. (2000). Actin-dependent propulsion of endosomes and lysosomes by recruitment of N-WASP. J. Cell Biol. *148*, 519–530.

Thompson, H.M., Skop, A.R., Euteneuer, U., Meyer, B.J., and McNiven, M.A. (2002). The large GTPase dynamin associates with the spindle midzone and is required for cytokinesis. Curr. Biol. *12*, 2111–2117.

Vanzo, N., Oprins, A., Xanthakis, D., Ephrussi, A., and Rabouille, C. (2007). Stimulation of endocytosis and actin dynamics by Oskar polarizes the *Drosophila* oocyte. Dev. Cell *12*, 543–555.

Velarde, N., Gunsalus, K.C., and Piano, F. (2007). Diverse roles of actin in *C. elegans* early embryogenesis. BMC Dev. Biol. *7*, 142.

Watts, J.L., Etemad-Moghadam, B., Guo, S., Boyd, L., Draper, B.W., Mello, C.C., Priess, J.R., and Kemphues, K.J. (1996). par-6, a gene involved in the establishment of asymmetry in early *C. elegans* embryos, mediates the asymmetric localization of PAR-3. Development *122*, 3133–3140.

White, J.G., Squirrell, J.M., and Eliceiri, K.W. (2001). Applying multiphoton imaging to the study of membrane dynamics in living cells. Traffic *2*, 775–780.

Wissler, F., and Labouesse, M. (2007). PARtners for endocytosis. Nat. Cell Biol. *9*, 1027–1029.

Wokosin, D.L., Squirrell, J.M., Eliceiri, K.W., and White, J.G. (2003). Optical workstation with concurrent, independent multiphoton imaging and experimental laser microbeam capabilities. Rev. Sci. Instrum. *74*, 193–201.

Zerial, M., and McBride, H. (2001). Rab proteins as membrane organizers. Nature reviews *2*, 107–117.